Available online at www.sciencedirect.com

ScienceDirect

Procedia Computer Science 2 (2010) 265–271

Procedia Computer Science

www.elsevier.com/locate/procedia

ICEBT 2010

Majority Voting based Classification of Thyroid Carcinoma

B.Gopinath[a,*], Dr.B.R.Gupta[b]

[a]*Research Scholor, Anna University of Technology, Coimbatore, India*
[b]*Research Supervisor, Anna University of Technology, Coimbatore, India*

Abstract

This paper presents the classification of Papillary carcinoma and Medullary carcinoma cells in Fine Needle Aspiration Biopsy (FNAB) microscopic cytological images of thyroid nodules under varying staining conditions. Initially image segmentation is performed to remove the background staining information in microscopic images using mathematical morphology. Feature extraction is carried out by Discrete Wavelet Transform (DWT) and Gray Level Co-occurrence Matrix (GLCM) and the classification is done using k-Nearest Neighbor (kNN) classifier. The DWT reports the maximum diagnostic accuracy of 97.5% while GLCM reports the diagnostic accuracy of 75.84%. However the diagnostic accuracy of GLCM has been improved as 90% by implementing the majority voting rule.

*Keywords:*Classification, Feature Extraction, Segmentation, Thyroid, Wavelet

1. Introduction

The thyroid is one of the largest glands in the body that regulates the rate of metabolism by producing thyroid hormones. The unwanted growth of cells on the thyroid forms a mass of tissue that is called as thyroid nodules. Most of these thyroid nodules are benign and not cancerous. Only 10-15% of all thyroid nodules are discovered to be thyroid cancer i.e. malignant. There are four main varieties of thyroid cancer namely Papillary carcinoma, Follicular carcinoma, Medullary carcinoma and Anaplastic carcinoma [1, 2].

Thyroid cytopathology is used as screening tool to detect cancer in its early stage by studying the cytological features of cancer affected cells in a given sample. Although screening leads to an earlier diagnosis, over-diagnosis and misdiagnosis are the negative effects of screening. Sometimes, cell boundaries are not well distinguishable due to poor dye quality and two or more cells may overlap which mislead the classification. While examining such samples, a pathologist assesses the changes in the distribution of the cells across the sample under examination and gives the diagnostic report. However, this judgment may lead to considerable variability. To overcome these problems and improve the reliability of diagnosis, it is necessary to develop efficient automated methods for performing the segmentation of cancer cells from the FNAB microscopic images and classifying benign, malignant and type of malignant using image processing techniques.

The researchers are very much interested in the automated Computer Aided Diagnosis (CAD) system for the classification of cancer cells in microscopic images to improve the diagnosis results. The research efforts have been directed in the field of medical image analysis to assist in diagnosis of cancer in various forms [3, 4, 5, 6, 7, 8, 9].

The proposed research work aims to segment the cancer cells in FNAB microscopic images of papillary carcinoma and medullary carcinoma of thyroid nodules with the help of mathematical morphology in order to classify cell types. Then the statistical textural features are extracted using two-level Discrete Wavelet Transform decomposition and Gray Level Co-occurrence Matrix and classification of cancer cells is carried out by k-nearest neighbor classifier with majority voting rule.

* Corresponding author. Tel.: +91-422-266-6264; fax: +91-422-266-5138.
E-mail address: gopiksr@rediffmail.com.

1877-0509
doi:10.1016/j.procs.2010.11.034

Majority voting rule is implemented to improve the diagnostic accuracy at the end of classification stage. We begin with introduction of fine needle aspiration biopsy in Section 2. The mathematical morphology based image segmentation method is described in Section 3. Section 4 describes the two-level DWT decomposition and GLCM based feature extraction. The kNN classification method and majority voting rule are presented in Section 5 and Section 6. Finally, the results and conclusion are summarized in Section 7 and 8.

2. Fine Needle Aspiration Biopsy

Fine Needle Aspiration Biopsy is the non-surgical method of determining benign or malignant state of the thyroid nodule. Thyroid FNAB can be performed in a general hospital by a doctor. Thyroid samples from the thyroid nodule are extracted using a 25-gauge needle with disposable 10-cc syringe by the doctor. The material collected from the FNAB is sent to the pathology laboratory. The pathologist examines the thyroid cells under a microscope based on the cytological features. After examination, the pathologist issues a cytological diagnosis report. The classifications are Benign, Malignant, Suspicious and Inadequate. Normally the accuracy of FNAB technique is around 95% and false negative and false positive results vary from 0-5% [1, 2].

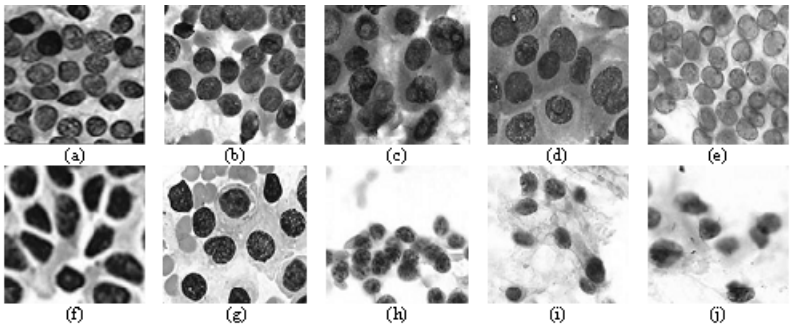

Fig.1 (a) to (e) Papillary carcinoma and (f) to (j) Medullary carcinoma training images

Fig. 1 shows the selected portions of FNAB cytological microscopic images of papillary carcinoma and medullary carcinoma of thyroid nodules which are used as training set images in our work [10]. Fig. 1(a) shows a DQ stained, 200X magnified FNAB images of Papillary carcinoma; (b), (c) and (d) show DQ stained, 400X magnified FNAB images of Papillary carcinoma; (e) shows Pap stained, 400X magnified FNAB images of Papillary carcinoma; (f) shows DQ stained, 200X magnified FNAB images of Medullary carcinoma; (g) shows DQ stained, 400X magnified FNAB images of Medullary carcinoma; (h) and (i) show Pap stained, 400X magnified FNAB image of Medullary carcinoma; (j) shows Congo Red stained, 400X magnified FNAB image of Medullary carcinoma of Thyroid nodule.

Our research work focuses on automated classification of type of malignant carcinoma in Thyroid FNAB cytological images using feature based image processing techniques. Fig. 2 shows the test images which are to be classified.

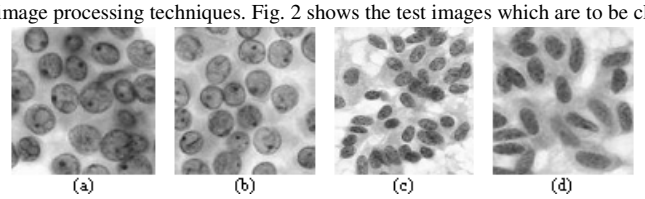

Fig.2 (a) and (b) Papillary and (b) and (c) Medullary carcinoma test images

3. Image Segmentation

The analysis of medical images comprises three basic steps: Segmentation of region of interest, Feature extraction and Classification. The classification accuracy is mainly depending on the efficient segmentation methodology. In our work, we have used mathematical morphology to segment the appropriate regions of medullary and papillary carcinoma cells in FNAB images. The small unwanted noise objects around the cells and small holes inside of cells in the image are removed by the morphological erosion and dilation based opening and closing operators [7, 11, 12].

The disk shaped structuring elements with radius of 1 and 8 pixels are used. If sets *I* and *Se* are referred to as the input image and structuring element respectively and *s* is an element of *Se*, then erosion is defined as the result of intersection of *s* and *I*. According to erosion operation, if all black elements in the structuring element match the neighbors of a pixel, then the original pixel becomes black, if not it becomes white.

$$I \Theta Se = \bigcap_{s \in Se} I_{-s} \tag{1}$$

Similarly, dilation is defined as the result of union of *s* and *I*. According to dilation operation, if at least one black element in the structuring element matches to a neighbor pixel, the original pixel becomes black, if not it becomes white.

$$I \oplus Se = \bigcup_{s \in Se} I_{s} \tag{2}$$

Based on erosion and dilation, two secondary morphological operators open and close are used. Erosion followed by dilation is called opening while dilation followed by erosion is called closing. The opening and closing operations are implemented by rolling the structuring element about inside and outer boundaries of the image respectively. Fig. 3 shows the results of papillary and medullary carcinoma images of morphology segmentation method.

$$Open : (I \circ Se) = (I \Theta Se) \oplus Se$$

$$Close : (I \bullet Se) = (I \oplus Se) \Theta Se \tag{3}$$

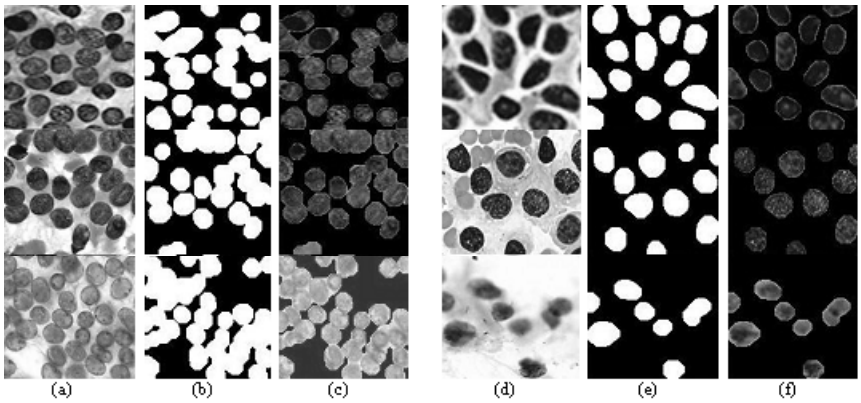

Fig. 3 (a) Input papillary carcinoma images; (b) Output images of Morphological open and close; (c) Segmented and superimposed output images; (d) Input medullary carcinoma images; (e) Output images of Morphological open and close; (f) Segmented and superimposed output images

4. Feature Extraction

Feature extraction is a method of generating description of an object in an image in terms of measurable values. The extracted features represent the properties of the object. These features can be used with a classifier to assign the class for the object.

4.1. Wavelet Decomposition

A large variety of feature extraction methods exist among which wavelet filtering is one such method that can be successfully used for feature extraction in texture analysis. In our work, we have used a simple Discrete Wavelet Transform representation. Among one-level and two-level DWT decomposition, we have used two-level DWT for extracting statistical textural features [13]. In two-level decomposition, the image is divided into four sub-bands using separable filters. Each coefficient in the sub-bands LL2, LH2, HL2, and HH2 represents a spatial area corresponding to approximately a 4×4 area of the original image. If

further decompositions are needed, LL2 can be used. The decomposition continues until an appropriate fine scale is reached. The representation of two-level decomposed image is shown in Fig. 4.

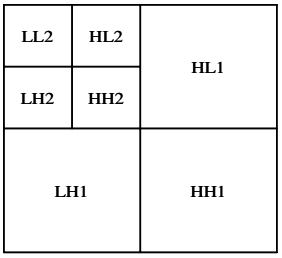

Fig. 4 Two-level Wavelet Decomposition

The Papillary and Medullary carcinoma training images are decomposed using 2-level DWT. The statistical features entropy, mean, standard deviation and variance of the sub-bands of two-level decomposed images are calculated and stored in feature library. The mean value of the image is defined as the average value of the image gray levels. It gives a measure of brightness. The standard deviation gives a measure of contrast. Variance is the square of standard deviation. It is the measure that gives us by how much the gray levels of the image are varying from the mean. Entropy measures the non-uniformity of an image and it achieves its largest value when the image is not texturally uniform.

$$Mean\ (\mu) = \sum_i \sum_j f(i,j)/N \tag{4}$$

$$Standard\quad Deviation\ \ (\sigma) = \sum_i \sum_j ((f(i,j)-\mu)^2/N)^{1/2} \tag{5}$$

$$Variance\ \ (V) = \sigma^2 \tag{6}$$

$$Entropy\ \ = -\sum_i \sum_j f(i,j)\log f(i,j) \tag{7}$$

where, $f(i,j)$ is the gray level value for each pixel and N is the total number of pixels in the region of interest. A set of five papillary and five medullary carcinoma images are involved in feature extraction. Since each image is cropped into four sub-images, the total number of images for training set becomes 40. After feature extraction, the total number of features becomes 160 among which mean, standard deviation, variance and entropy are 40 each.

4.2. Gray Level Co-occurrence Matrix

Gray Level Co-occurrence Matrix is a texture analysis method that is used for estimating image properties in terms of statistical features. GLCM computes the relation between two neighbouring pixels, where the first pixel is called reference and the second is the neighbour pixel. In order to estimate the similarity between different gray-level co-occurrence matrices 14 statistical features are addressed in the literature [14, 15].

To reduce the computational complexity, only three of these features have been selected. The derived features are homogeneity, energy and contrast. Energy, also called uniformity, is a measure of textural uniformity of an image. Energy reaches its highest value when gray level distribution has either a constant or a periodic form. The GLCM homogeneity measures the closeness of the distribution of elements in the GLCM to the GLCM diagonal. The GLCM homogeneity of an image object is high if GLCM concentrates along the diagonal. Contrast is a measure of the amount of local variations in the grey-level co-occurrence matrix [14].

$$Contrast = \sum_{i,j=0}^{N-1} P_{i,j}(i-j)^2 \tag{8}$$

$$Homogeneity = \sum_{i,j=0}^{N-1} \frac{P_{i,j}}{1+(i-j)^2} \tag{9}$$

$$Energy = \sum_{i,j=0}^{N-1} P_{i,j}{}^2 \tag{10}$$

Where, i and j are coordinates of the co-occurrence matrix, $P_{i,j}$ is element in the co-occurrence matrix at the coordinates i and j, N is dimension of the co-occurrence matrix.

5. *k*-Nearest Neighbor Classifier

The *k*-nearest neighbor (kNN) algorithm is one of the most widely used machine learning algorithms for pattern classification. The kNN is used for classifying patterns based upon the closest training samples in the feature space. In kNN algorithm, the entire training set is stored in feature library. To classify an unlabeled test image, the distance is computed between the feature of test image and each stored feature of training image and the test image is assigned the class of the nearest neighboring image. The performance of a kNN classifier is determined by the choice of k and the distance metric used. Among all distance metrics, Euclidean distance is the commonly used measurement. A large value of k can be selected if the size of the training data set is large and vice versa [16, 17].

The classification problem is solved in two phases: training phase and testing phase. In training phase, DWT and GLCM are applied on labeled training images of papillary and medullary carcinoma. The statistical features mean, standard deviation, variance and entropy are calculated using DWT while homogeneity, energy and contrast are calculated using GLCM and stored in the feature library. In the testing phase, both the feature extraction methods are again applied on the unlabeled test images of papillary and medullary carcinoma and similar set of statistical features are extracted. Then these extracted features are compared with the feature library and classified using kNN classifier with majority voting rule. The training and testing phases are explained in Fig. 5 and Fig. 6.

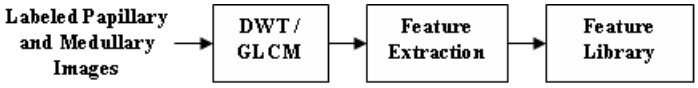

Fig. 5 Training Phase with labelled images

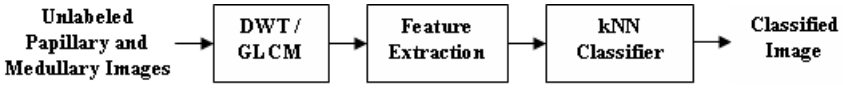

Fig. 6 Testing Phase with unlabelled image

6. Majority Voting Rule

The majority voting rule is normally used to find a particular member in any given sequence which has more votes than all the others. This searching rule has been used in association with kNN classifier to improve the diagnostic accuracy of our classification problem. In our work, we are using two test sets of papillary and medullary carcinoma images P1M1 and P2M2. Since each image is cropped into four sub-images, the total number of images for testing set becomes 16. When the test image P1 undergoes for classification, the four sub-images of P1 will be assigned with new labels. The possible labels are (Papillary; Papillary; Papillary; Papillary) or (Medullary; Papillary; Papillary; Papillary), and so on. Now we are searching for majority number of labels to assign a new label for the image P1. If we have four or three similar labels of Papillary, then the P1 image is assigned with the label 'Papillary'. The same rule is implemented for all the testing images so that the diagnostic accuracy can be improved.

7. Results and Observations

The classification results are presented in Table 1 and Table 2. The available training set images are divided into five groups as Training Set 1 through Training Set 5. Each training set comprises eight images among which four are papillary carcinoma and four are medullary carcinoma images. Therefore total number of images for training phase becomes 40 images. These 40 images are trained and statistical textural features are extracted using DWT and GLCM and stored in feature library. In testing phase, two sets of 4 images of papillary and medullary carcinoma images P1M1 and P2M2 are used. The unlabeled test images which are to be classified as either papillary carcinoma or medullary carcinoma are also given as input images to feature extraction phase. The similar features are again extracted and the features are compared with feature library. Papillary carcinoma is tested for positive test while medullary carcinoma is tested for negative test. There are two and three false negative results for

P1M1 and P2M2 test images due to entropy, contrast and energy of training set 1 and training test 3 respectively. But there is only one false positive result for both P1M1 and P2M2 test images due to homogeneity of training set 2 as shown in Table 1.

Table 2 and Fig. 7 give the comparison results of diagnostic accuracies with and without majority voting rule. The maximum diagnostic accuracy of 97.5% is achieved using discrete wavelet transform and minimum diagnostic accuracy of 75.84% is obtained from Gray Level Co-occurrence Matrix for various testing sets of FNAB cytological images of thyroid nodules. However the minimum diagnostic accuracy has been improved from 75.84% to 90% by implementing majority voting rule.

Table 1: Diagnostic results

Test Images	Papillary (Positive Test)		Medullary (Negative Test)	
	True Positive	False Negative	True Negative	False Positive
P1M1	33	2 (Entropy, Contrast)	34	1 (Homogeneity)
P2M2	32	3 (Entropy, Contrast, Energy)	34	1 (Homogeneity)

Table 2: Comparison of diagnostic accuracy

Feature Extraction	Accuracy without majority voting		Accuracy with majority voting	
	P1M1	P2M2	P1M1	P2M2
DWT	97.50	97.50	97.50	97.50
GLCM	88.34	75.84	93.34	90.00
DWT+GLCM	93.57	88.21	95.71	94.29

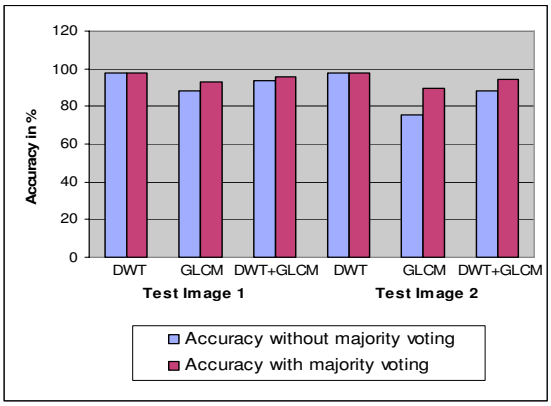

Fig. 7 Comparison of diagnostic accuracy

8. Conclusion

We have done the implementation of majority voting rule based image classification method to perform the classification of Papillary and Medullary carcinoma in FNAB cytological images of thyroid nodules. The maximum diagnostic accuracy of 97.5% is achieved using Discrete Wavelet Transform and minimum diagnostic accuracy of 75.84% is obtained from Gray Level Co-occurrence Matrix for various testing sets of FNAB cytological images of thyroid nodules. However the minimum diagnostic accuracy of GLCM has been improved from 75.84% to 90% by implementing majority voting rule.

References

[1] S.A.Mahar, A.Husain A., and N.Islam, Fine needle aspiration cytology of thyroid nodule: Diagnostic accuracy and pitfalls, Journal of Ayub Medical College, Abbottabad, 18(4) (2006) 26-29.

[2] Suresh Kumar, Shakil Aqil and Abdullah Dahar, Role of Fine Needle Aspiration Cytology in thyroid diseases, International Journal of Surgery, Pakistan, 13(1) (2008).22-25.

[3] M.El.Adawy, Z.Shehab, H.Keshk and M.El.Shourbagy, A Fast Algorithm for Segmentation of Microscopic Cell Images, International conference on Information & Communication Technology, (2006).

[4] A.Daskalakis, S.Kostopoulos, P.Spyridonos, D.Glotsos, P.Ravazoula, M.Kardari, I.Kalatzis, D.Cavouras and G.Nikiforidis, Design of a multi-classifier system for discriminating benign from malignant thyroid nodules using routinely H&E-stained cytological images, Computers in Biology and Medicine, 38 (2008) 196-203.

[5] C.Duanggate, B.Uyyanonvara, and T.Koanantakul, A Review of Image Analysis and Pattern Classification Techniques for Automatic PAP Smear Screening Process, International Conference on Embedded Systems and Intelligent Technology, (2008) 212-217.

[6] B.Gopinath and B.R.Gupta, Isolation of Thyroid Cancer Cells in FNAB Images using Image Processing Techniques, International Journal of Applied Engineering Research, 5 (1) (2010), 167-175.

[7] M.Hrebien, P.Stec, T.Nieczkowski and A.Obuchowicz, Segmentation of Breast Cancer Fine Needle Biopsy Cytological Images, International Journal of Applied Mathematics and Computer Science, 18(2) (2008) 159-170.

[8] M.Sarkar and T.Y.Leong, Application of k-Nearest Neighbors Algorithm on Breast Cancer Diagnosis Problem, Australasian Physical & Engineering Science in Medicine, 26 (1) (2009) 6-11.

[9] T.E. Schneider, Automated Classification of Analysis and Reference Cells in Microscopic Images for Cancer Diagnostics, Proceedings of the 11th International Student Conference on Electrical Engineering POSTER, (2007)1-5.

[10] Cytopathology on-line teaching resource of the Johns Hopkins University, Balitmore, MD.

[11] R.C.Gonzalez and R.E.Woods, Digital Image Processing, 2nd ed., Pearson Education, Inc., (2002).

[12] B.Gopinath and B.R.Gupta, A Comparative Study of Region-based Image Segmentation Methods for extracting Dead Cancer Cells in Microscopic Cytological Image, Proceedings of the International Conference on Biomedical Instrumentation and Health care Engineering, Chennai, India, (2009) 6-12.

[13] S.Arivazhagan and L.Ganesan, Texture Classification using Wavelet Transform, Pattern Recognition Letters, 24(9-10) (2003) 1513-1521.

[14] R.M.Haralick, K.Shanmugam, and I.Dinstein, Textural Features for Image Classification, IEEE Transactions on Systems, Man, and Cybernetics, 3(6) (1973) 610-621.

[15] M.Partio, B.Cramariuc, M.Gabbouj, and A.Visa, Rock Texture Retrieval Using Gray Level Co-Occurrence Matrix, Proceedings of the 6th Nordic Signal Processing Symposium, Finland, (2004).

[16] Z.Bodo and Z.Minier, On Supervised and Semi-supervised k-Nearest Neighbor Algorithms, 7th Joint Conference on Mathematics and Computer Science, Romania, (2008) 1.

[17] Q.Hu, D.Yu and Z.Xie, Neighborhood classifiers, Expert Systems with Applications, 34 (2008) 866–876.